The Prolate Spheroid Separates Turbulence Models

By Sung-Eun Kim, Principal Development Engineer, and Shin H. Rhee, Senior Consulting Engineer, Fluent Inc.; and Davor Cokljat, Senior Principal Developer, Fluent Europe Ltd.

Contours of the normalized invariant of the deformation tensor in a cross-flow plane toward the rear of the spheroid; the RSTM-2 model was used with an incidence angle of 20°

Abbrev.	Description
SA	Spalart-Allmaras
KO-1	High-Re k-ω
KO-2	Low-Re k-ω
SST	Blended k-ω
RSTM-1	Baseline Reynolds stress transport model
RSTM-2	RSTM-1 with a modified ε equation
RSTM-3	RSTM-1 with another modified ε equation

Table 1: Turbulence models used in this study; see Reference 3 for more details

DESPITE ITS SIMPLE GEOMETRY, the flow around a prolate spheroid at incidence offers a rich gallery of complex three-dimensional turbulent shear flows, featuring stagnation flow, a highly three-dimensional boundary layer under the influence of strong pressure gradients and streamline curvature, cross-flow separation, and the formation and evolution of free-vortex sheets and stream-wise vortices. All of these features are the archetypes of flows around airborne and underwater vehicles at incidence or in maneuvering, so they have been the basis of much research over the years. A number of experimental studies (1, 2) have provided comprehensive data that reveals the salient physics of the flow. A recent numerical study at Fluent, conducted on a 6:1 prolate spheroid using incidence angles of α = 10°, 20°, and 30°, made use of some of the literature data for the purpose of validating turbulence models. Turbulence modeling plays a significant role here, in light of the challenging features noted above, so several popular engineering turbulence models with good track records for similar flows were evaluated, including the Spalart-Allmaras model, a family of k-ω models, and a variety of Reynolds stress transport models. All of the computations were carried out using FLUENT.

The seven turbulence models used in the study are outlined in Table 1 (3). In addition to the one-equation Spalart-Allmaras (SA) model, three variants of the k-ω model in popular use today were also used. The first two (KO-1 and KO-2) are suitable for high and low Reynolds number flows, respectively. The third, often referred to as the shear-stress transport (SST) k-ω model, is essentially a two-zone model that blends a variant of the k-ω model in the inner boundary layer with a transformed version of the traditional k-ε model in the outer boundary layer. A baseline Reynolds-stress transport model (RSTM-1) showed substantial improvements over linear k-ε model predictions made in the past, but fell short of expectations in this study. Thus two other RSTM approaches, each with modified ε equations and designated RSTM-2 and RSTM-3, were also evaluated.

A fine mesh was used for simulations involving the SA, SST, KO-1, and KO-2 models, all of which can be naturally integrated to wall. All other computations were performed using a coarser mesh and wall functions.

A visual impression of the mean flow in question is portrayed by pathlines around the spheroid for the α = 30° case. The pathlines highlight the most prominent features of the flow, such as crossflow in the boundary layer, a free vortex sheet, and stream-wise vortices. Taken together, these phenomena are an embodiment of cross-flow separation, which is significant because the structure of the separation and its change with incidence angle greatly affect the maneuvering characteristics of the body.

The normalized invariant of the deformation tensor, which identifies regions where a particular flow is mostly shear-dominated ($D \rightarrow 0$), strain-dominated ($D \rightarrow 1$), or rotational ($D \rightarrow -1$), can also be used to gain insight about a flow field. On a cross section of the spheroid, about 2/3 of the length from the leading edge with a 20° incidence angle, the normalized invariant shows that the flow is largely shear-dominated throughout the boundary layer, and predominantly rotational near the core of the stream-wise vortices on the leeward side. In general, rotation

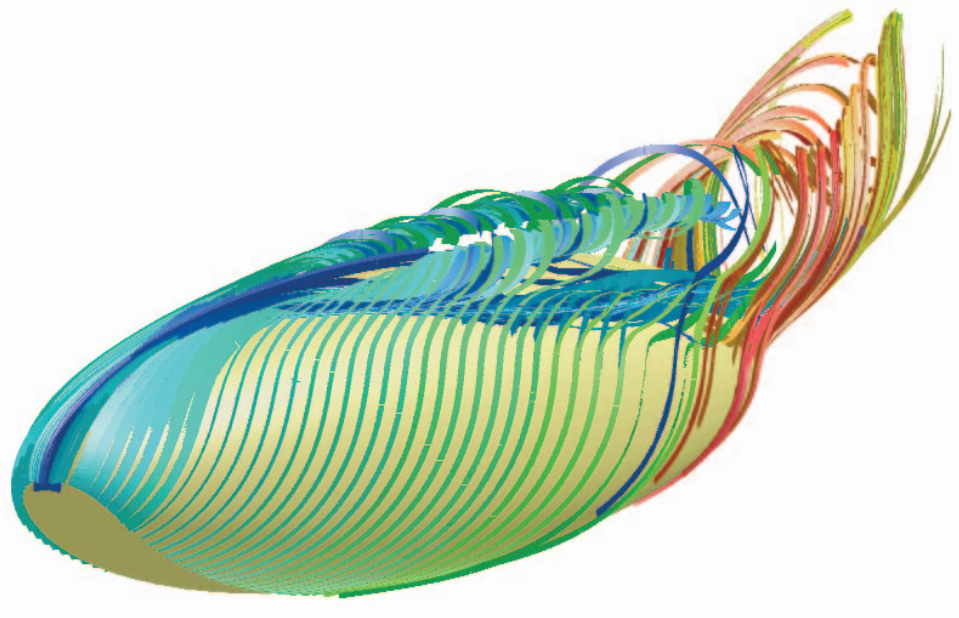

Cross-flow separation and streamwise vortices on a 6:1 prolate spheroid at an incidence angle of 30°

inhibits the energy transfer from larger to smaller turbulent eddies, decreasing the decay rate of the turbulent kinetic energy (4). When a mean shear exists, rotation can either delay or accelerate the energy transfer depending on the relative orientations of the mean shear and rotation, attenuating or accentuating turbulence accordingly. Effects such as these place heavy demands on turbulence models in complex flow situations.

While three angles of attack were simulated, the surface quantities were found to exhibit much richer features at $\alpha = 20°$, and the differences between the models also became far more noticeable. The circumferential distribution of surface pressure, C_p, at $\alpha = 20°$ can be used to illustrate the differences between the SA, SST, KO-1 and KO-2 models using the fine mesh. The experimental data (1, 2) show that the primary vortex is located near $\varphi = 158°$ in the crossflow planes at both x/L = 0.6 and 0.772, where conspicuous dips in the measured C_p data occur. The KO-2 model captures both the location and magnitude of the minimum C_p better than the others. At x/L = 0.772, it also captures the small kink caused by a secondary vortex above the surface, detected at $\varphi = 140°$ in the experiment. Evidently, the low-Reynolds number modification in the KO-2 model seems to play a significant role in improving the results predicted by this model. The SST model gives only marginally better results than the SA model, and falls behind the KO-1 and KO-2 models.

The distributions of C_p at $\alpha = 20°$ predicted using the SST and KO-1 models on the coarse mesh were found to be only marginally different from the predictions made from the fine mesh. This finding is quite significant, inasmuch as it gives a credential to the wall function approach and the results based thereupon. On the coarse mesh, the baseline RSTM-1 model performs clearly better than the SST model, but not as well as the KO-1 model. The RSTM-2 and RSTM-3 models, however, bring remarkable improvements over the RSTM-1 model, outperforming all of the k-ω models. It is interesting to note that seemingly minor changes in the ε equation lead to such disproportionately large differences in the results.

The improvements gained by using the RSTM-2 and RSTM-3 models for the prediction of surface quantities such as C_p are directly carried over to the predictions of force and moment. For slender bodies like prolate spheroids, there is a nonlinear increase of lift with incidence angle, due to the low pressure near the cores of vortices that is impressed upon the nearby body surface. Accurate prediction of the location and strength of the vortices is therefore prerequisite to successful prediction of the forces and moments. Using the coarse mesh, the lift prediction by the RSTM-1 model is largely comparable to that from the SST and KO-1 models. The RSTM-2 and RSTM-3 results, however, are in better agreement with the data. ■

References:

1 C.J. Chesnakas, R.L. Simpson, *AIAA J.* **1997**, *35*, 990-999

2 T.G. Wetzel, R.L. Simpson, C.J. Chesnakas, *AIAA J.* **1998**, *36*, 557-564.

3 S.E. Kim, S.H. Rhee, D. Cokljat, *AIAA Paper* **2003**, no. 2003-0429.

4 R.A. Wigeland, H.M. Nagib, IIT Fluids & Heat Transfer Report, R78-1, 1978.

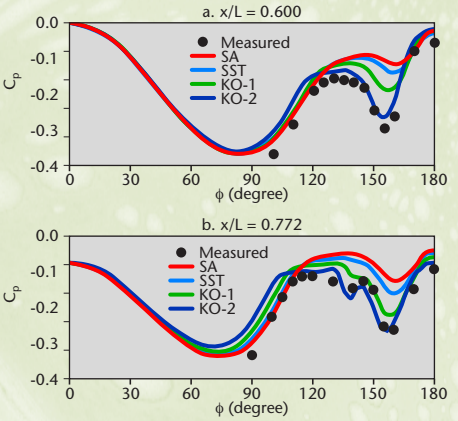

Surface pressure coefficient, Cp, at two axial locations computed on the fine mesh for an incidence angle of 20°, showing a comparison of the SA, SST, KO-1, and KO-2 turbulence models with experiment

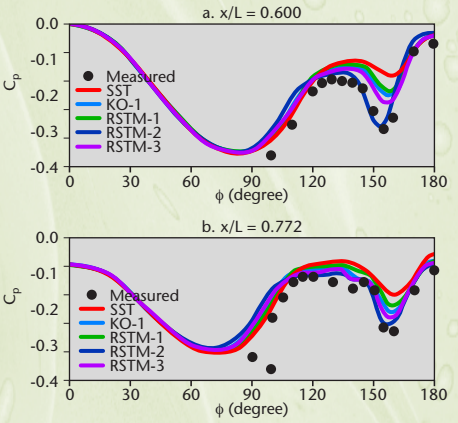

Surface pressure coefficient, Cp, at two axial locations computed on the coarse mesh (using wall functions) for an incidence angle of 20°, showing a comparison of the SST, KO-1, and RSTM turbulence models with experiment

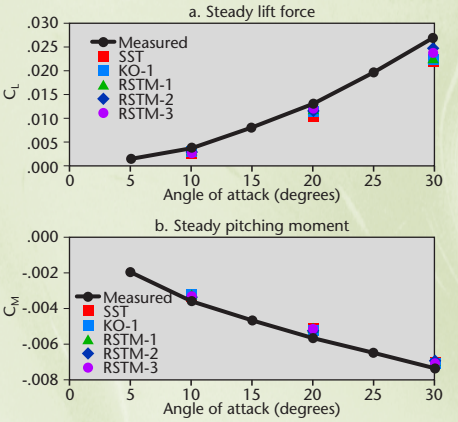

Lift (C_L) and pitching moment (C_M) predictions made using the coarse mesh (using wall functions), showing a comparison of the SST, KO-1, and RSTM turbulence models with experiment